Geometrical Picture of Dynamical Facilitation†

Stephen Whitelam‡ and Juan P. Garrahan*,‡,§

Theoretical Physics, University of Oxford, 1 Keble Road, Oxford, OX1 3NP United Kingdom, and School of Physics and Astronomy, University of Nottingham, Nottingham, NG7 2RD United Kingdom

Received: November 30, 2003; In Final Form: January 27, 2004

Kinetically constrained models (KCMs) are models of glass formers based on the concept of dynamic facilitation. This concept accounts for many of the characteristics of the glass transition. KCMs usually display a combination of simple thermodynamics and complex glassy dynamics, the latter being a consequence of kinetic constraints. Here we show that KCMs can be regarded as systems whose configuration space is endowed with a simple energy surface but a complicated geometry. This geometry is determined solely by the kinetic constraints and determines the dynamics of the system. It does not affect the overall distribution of states. Low-temperature dynamical slow-down is then a consequence of the competition between the paths allowed by the geometry of configuration space and those leading to energy relaxation. This competition gives rise to dynamical bottlenecks unrelated to static properties. This view of the dynamics is distinct from that based on an underlying static rugged energy landscape. We illustrate our ideas with simple examples.

1. Introduction

The view of the glass transition (see refs 1−3 for general reviews) as a dynamical phenomenon emerges naturally from the real-space picture of supercooled liquids developed in refs 4−8. This work demonstrates that many of the properties of supercooled liquids can be simply explained by the existence and statistical properties of spatially correlated dynamics or dynamical heterogeneity.[9−11] Dynamical heterogeneity has been observed both in deeply supercooled liquids,[12] in the mildly supercooled regime in simulations,[13] and in experiments on colloidal suspensions.[14]

Heterogeneous dynamics, in combination with structural homogeneity, as observed in glass formers, appears in systems possessing both localized excitations and facilitated dynamics.[15−17] The concept of dynamic facilitation stipulates that the dynamics of a local region is suppressed if it is bordered by immobile regions and thus reflects the idea that particles in a jammed liquid cannot rearrange unless adjacent to mobile particles. Dynamic facilitation is realized in KCMs, which are simple models of non interacting particles or excitations in a lattice whose dynamics is subject to kinetic constraints (see ref 18 for a review). Examples of KCMs are spin facilitated models, like the Fredrickson−Andersen (FA) model[17] or the East model,[19] and constrained lattice gases, such as the Kob−Andersen model.[20]

In this paper, we study the effect that dynamic facilitation has on the geometry of configuration space and how in turn this affects the dynamics.[21] We show, by generalizing KCMs to continuous degrees of freedom, that kinetic constraints impose a metric structure on configuration space which does not affect the static distribution of states, and therefore the thermodynamics, but which has a dramatic effect on the paths between states at low energies. We show that dynamical slow-down at low temperatures occurs because the system is forced to evolve along configuration space paths of least metric distance, or geodesics, which are distinct from the paths that relax the energy. This competition between available trajectories and energy relaxation gives rise to dynamical barriers, or bottlenecks, which are unrelated to the statics of the system. This view of the dynamics is distinct from that based on the idea that a static rugged energy landscape is responsible for the properties of glass formers (see e.g. ref 3).

This paper is organized as follows. In section 2, we discuss the geometric interpretation of dynamic facilitation. In sections 3 and 4, we illustrate our ideas with simple examples. In section 5, we state our conclusions.

2. Geometrical Interpretation of Constrained Dynamics

The real-space picture of supercooled liquids of refs 4, 5, 6, and 8 is based on two observations. First, at low temperature, very few particles in the liquid are mobile, and these mobility excitations are localized in space. Second, regions of the liquid cannot become mobile unless their neighboring regions are mobile. These observations are implemented as follows. A supercooled fluid in d spatial dimensions is coarse-grained into cells of linear size of the order of the static correlation length as given by the pair correlation function. Cells are classified by a scalar mobility field, x, identified by coarse-graining the system on a microscopic time scale. Mobile regions carry a free energy cost, and when mobility is low, interactions between cells are not important. Adopting a thermal language, we expect static equilibrium to be determined by the noninteracting Hamiltonian

$$H[x] = \sum_{\mu=1}^{N} f_\mu(x^\mu) \tag{1}$$

where $\mu = 1, ..., N$ labels the lattice site, x^μ is the mobility field at site μ, and f_μ is an analytic function of x^μ chosen so that the ground state of the model is such that $|x^\mu|$ is small. At low mobility, the distinction between single and multiple occupancy is irrelevant, as is the distinction between discrete or continuous

† Part of the special issue "Hans C. Andersen Festschrift".
* To whom correspondence should be addressed.
‡ University of Oxford.
§ University of Nottingham.

10.1021/jp037653x CCC: $27.50
Published on Web 02/27/2004

degrees of freedom. In what follows, we assume x^μ to be real. The dynamics of the mobility field is given by a master equation

$$\partial_t P(x, t) = \sum_\mu \mathcal{C}_\mu(x) \mathcal{L}_\mu P(x, t) \tag{2}$$

where $P(x, t)$ is the probability that the system has configuration $x \equiv \{x^\mu | \mu = 1, 2, ..., N\}$ at time t. The local operators $\mathcal{L}_\mu$ are the same as those for unconstrained local dynamics. Their action on P can be written

$$\mathcal{L}_\mu P(x) = \sum_{x'^\mu} w(x'^\mu \to x^\mu)\, P\,(x'^\mu, \{x^{\nu\neq\mu}\}) - \sum_{x'^\mu} w(x^\mu \to x'^\mu)\, P\,(x^\mu, \{x^{\nu\neq\mu}\}) \tag{3}$$

where $w(x^\mu \to x'^\mu)$ is the probability of going from configuration $(x^\mu, \{x^{\nu\neq\mu}\})$ to configuration $(x'^\mu, \{x^{\nu\neq\mu}\})$ in unit time. We ensure a unique equilibrium configuration exists by requiring eq 2 to obey detailed balance with respect to eq 1, i.e.

$$\frac{w(x \to x')}{w(x' \to x)} = \mathrm{e}^{-\beta(H[x']-H[x])} \tag{4}$$

The kinetic constraint, $\mathcal{C}_\mu(x)$, is designed to suppress the dynamics of cell μ when surrounded by immobile regions. It must also be such that eq 2 satisfies a detailed balance, which is achieved if $\mathcal{C}_\mu(x)$ does not depend on x^μ itself. To reflect the local nature of dynamic facilitation, we allow $\mathcal{C}_\mu$ to depend only on the $\{x^\nu\}$ of nearest neighbors of μ and require that $\mathcal{C}_\mu$ is small when local mobility is scarce. Equations 1−4 define a generic KCM.

We now show that eq 2 has a simple geometrical interpretation. Using standard methods,[22] we pass from the master eq 2 to the Fokker−Planck equation

$$\partial_t P(x, t) = \sum_\mu \mathcal{L}_\mu^{(\mathrm{FP})} P(x, t) \tag{5}$$

where

$$\mathcal{L}_\mu^{(\mathrm{FP})} = \frac{\partial}{\partial x^\mu}\left\{ \mathcal{C}_\mu(x) f'_\mu(x^\mu) + T\frac{\partial}{\partial x^\mu}\mathcal{C}_\mu(x)\right\} \tag{6}$$

The prime on f_μ denotes differentiation with respect to x^μ. Equation 5 has a simple physical interpretation: it describes single-particle driven diffusion on an N-dimensional curved space $\{x^\mu | \mu = 1, 2, ..., N\}$. The form of the driving term in (6) comes from the Hamiltonian (1) and the kinetic constraint. However, the curvature of this space is due solely to the kinetic constraint: from the form of a Fokker−Planck equation on a curved manifold,[22] we identify the inverse metric tensor of this space as $g^{\mu\nu}(x) = \delta^{\mu\nu}\mathcal{C}_\mu(x)$. Thus, the metric reads

$$g_{\mu\nu}(x) = \delta_{\mu\nu}\mathcal{C}_\mu^{-1}(x) \tag{7}$$

No summation is implied. The effect of dynamic facilitation is to endow the configuration space x with a nontrivial metric. Since dynamic facilitation is responsible for the interesting dynamical properties of these models, we expect that these dynamical properties can be extracted from the metric tensor.

The effect of the metric on configuration space trajectories is made clearer by writing a formal solution to eq 5[23]

$$P(x_b, t_b | x_a, t_a) = \int_a^b \sqrt{|g|}\,\mathcal{D}x \mathrm{e}^{-\mathcal{J}[x]} \tag{8}$$

where $P(x_b, t_b | x_a, t_a)$ is the conditional probability that a system starting at point x_a in configuration space at time t_a is found at point x_b at time t_b. We have introduced the determinant of the metric, $|g| \equiv \det(g_{\mu\nu}) = \Pi_\mu \mathcal{C}_\mu^{-1}$. The path integral (8) is taken over all configurations of the system, weighted by the dynamic action $\mathcal{J}[x]$. Up to constant terms, this action reads

$$\mathcal{J}[x] = \frac{1}{T}(H[x_b] - H[x_a]) + \frac{1}{T}\int_{t_a}^{t_b} \mathrm{d}t \left(\dot{x}^\mu g_{\mu\nu}\dot{x}^\nu + \frac{\partial H}{\partial x^\mu} g^{\mu\nu}\frac{\partial H}{\partial x^\nu}\right) \tag{9}$$

where dots denote differentiation with respect to time, and the summation convention for once-repeated upper and lower indices is implied.

The action (9) weights the configuration space trajectories of our system. The system's classical trajectory, i.e., the path taken by the dynamics when $T \to 0$, is one of extremum $\mathcal{J}$. At finite T, stochastic fluctuations cause perturbations about this path. Equation 9 shows clearly the way the various ingredients of a dynamically facilitated model influence its trajectory through configuration space. The first term depends only on the Hamiltonian (1) evaluated at the endpoints. It gives rise to Boltzmann weights in the path integral (8) and plays no role in choosing the trajectory of the system. The path is chosen by a competition between the two terms in the integral of eq 9. The first term, $\mathcal{J}_1 \equiv T^{-1}\int \mathrm{d}t\, \dot{x}^\mu g_{\mu\nu}\dot{x}^\nu$, is purely geometrical. It is the action for free motion in a curved background. It depends on the metric $g_{\mu\nu}$ and, therefore, on $\mathcal{C}^{-1}$. The second term, $\mathcal{J}_2 \equiv T^{-1}\int \mathrm{d}t\, \partial_\mu H g^{\mu\nu}\partial_\nu H$, depends on the Hamiltonian (1) but is proportional to the inverse metric $g^{\mu\nu}$ and so to $\mathcal{C}$. At low temperatures, we expect $\mathcal{J}_2$ to be important only far from equilibrium, when mobility is plentiful, or equivalently when the magnitudes of the coordinates $|x^\mu|$ are large and $\mathcal{C}$ is large, and the system's relaxation will take place by way of gradient descent on the energy surface. When mobility has diminished significantly the constraints $\mathcal{C}$ become small. We then expect $\mathcal{J}_1$ to dominate. Hence the classical trajectory of the system in the region of weak dynamic facilitation will be governed by extremum $\mathcal{J}_1$. This corresponds to the equation of a geodesic[24]

$$\ddot{x}^\mu + \Gamma^\mu_{\alpha\beta}\dot{x}^\alpha\dot{x}^\beta = 0 \tag{10}$$

The Christoffel symbols $\Gamma^\mu_{\alpha\beta}$ are defined as $\Gamma^\mu_{\alpha\beta} \equiv 1/2\, g^{\mu\nu}(g_{\nu\alpha,\beta} + g_{\beta\nu,\alpha} - g_{\alpha\beta,\nu})$, and the metric tensor raises and lowers indices. Equation 10 tells us how the kinetic constraint controls the system's trajectory in configuration space in the dynamically constrained regime. When mobility is scarce, the constraint $\mathcal{C}$ is small, and the metric distance between points in configuration space, $s_{ab} \equiv \int_a^b (g_{\mu\nu}\, \mathrm{d}x^\mu\, \mathrm{d}x^\nu)^{1/2}$, is large by virtue of eq 7. By minimizing this distance, and so following eq 10, we expect the system to follow a path that does not lead directly to a configuration of lowest energy. This is a geometrical interpretation of dynamical arrest.

3. A Simple Example

We now illustrate these ideas with a simple example. We define a model of two variables, $\{x^\mu\} = \{x, y\}$, with each variable constraining the other. Although such a model cannot exhibit true glassiness, it is useful because we can visualize directly the two-dimensional configuration space it inhabits. We choose the Hamiltonian (1) to be quadratic

$$H = \frac{J}{2}(x^2 + y^2) \tag{11}$$

where J sets the energy scale. We choose the constraint functions

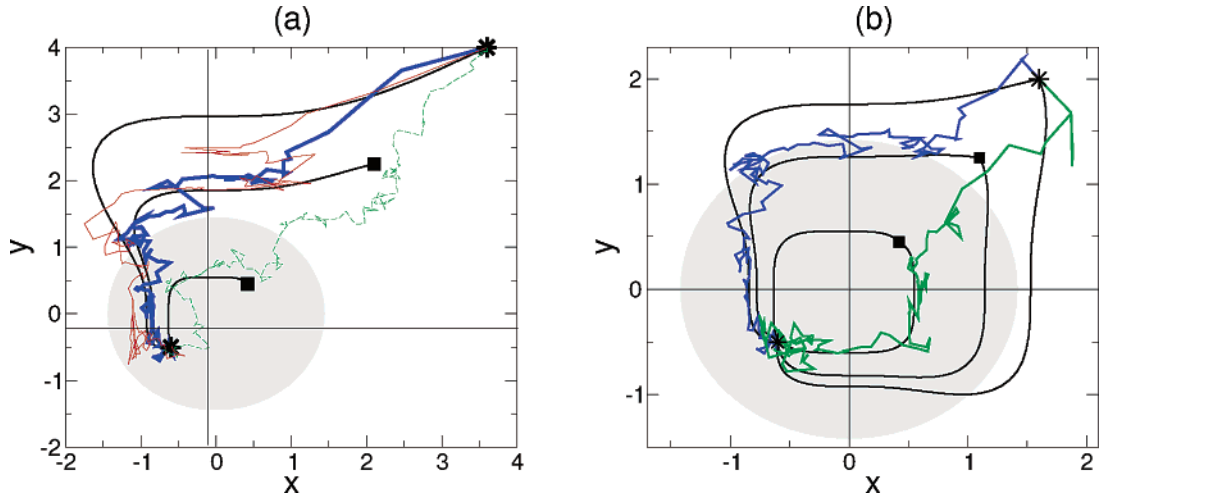

Figure 1. Configuration space trajectories for the toy model described in the text. Panel a: $T = 2.0$, $J = 1$, $t_b - t_a = 129$, $(x_a, y_a) = (3.6, 4.0)$, $(x_b, y_b) = (-0.6 \pm 0.01, -0.5 \pm 0.01)$. We used TPS with the Crooks−Chandler[27] algorithm to generate 2.78×10^8 trajectories, starting from point *a* (indicated by a star at the top right), of which 11 403 landed in the end-point *b* (indicated by a star at the bottom left). The thin red path is a representative trajectory. The thick blue path is the mean of those trajectories. The dashed green path is the mean of 273 trajectories reaching *b* from *a* for an unconstrained version of an otherwise identical model. Numerical solutions to the geodesic equation 14 joining *b* to three other points (shown as black squares) are overlaid. The gray circle encloses the equilibrium region $\langle x^2 + y^2 \rangle = T/J$. Panel (b): a similar plot starting from $(x_a, y_a) = (1.6, 2.0)$. Again, 2.78×10^8 trajectories were generated. The thick blue path shows the mean of 2199 trajectories landing in region *b* which follow the left-hand side route. The average path over 6 right-hand side trajectories is also shown in green.

to be quadratic also, with each coordinate constraining the other

$$\mathcal{C}_x = y^2, \ \mathcal{C}_y = x^2 \tag{12}$$

Thus, the Fokker−Planck eq 5 is determined. Equation 7 gives the metric of this system as

$$g_{\mu\nu} = \begin{pmatrix} 1/y^2 & 0 \\ 0 & 1/x^2 \end{pmatrix} \tag{13}$$

The metric is singular, and so distances in this configuration space become very large, when x or y vanish, reflecting the tendency of the kinetic constraint to suppress the dynamics of the system in the regime of low mobility. The space described by this metric is negatively curved with curvature scalar $R = -4(x^2/y^2 + y^2/x^2)$.[24] The geodesics follow from eq 10 which in this case read

$$y\ddot{x} + (y/x)^3\dot{y}^2 - 2\dot{x}\dot{y} = 0, \quad x\ddot{y} - (x/y)^3\dot{x}^2 - 2\dot{x}\dot{y} = 0 \tag{14}$$

To illustrate the effect of the kinetic constraint on the trajectories chosen by the system, we first cast eq 5 into a form more convenient for numerical simulation. In the usual way,[25] we recognize that eq 5 is equivalent to the coupled Langevin equations

$$\begin{pmatrix} \dot{x}(t) \\ \dot{y}(t) \end{pmatrix} = -\begin{pmatrix} Jy^2(t)x(t) \\ Jx^2(t)x(t) \end{pmatrix} + \begin{pmatrix} |y(t)|\eta_1(t) \\ |x(t)|\eta_2(t) \end{pmatrix} \tag{15}$$

where the Gaussian white noise variables $\eta_i(t)$ have zero mean and variance $\langle \eta_i(t)\eta_j(t') \rangle = 2T\delta(t - t')\delta_{ij}$. In this representation, the kinetic constraint manifests itself as a state dependent rate: the driving term is linear in $\mathcal{C}$ while the noise term goes as $\sqrt{\mathcal{C}}$. The unconstrained version of the same model, i.e., one for which $(\mathcal{C}_x, \mathcal{C}_y) = (1, 1)$, would have the Langevin equation $\dot{x}^\mu(t) = -Jx^\mu + \eta^\mu(t)$.

We now show explicitly that low-temperature trajectories with fixed initial and final configurations are approximated by the geodesic eq 14. We have used transition path sampling (TPS)[26] to ensure that we obtained a set of trajectories which both obeyed the endpoint conditions were well-sampled from the dynamical action (9). To generate out-of-equilibrium trajectories for the relaxation from high energy configurations, we used the Crooks−Chandler[27] algorithm; alternatives such as the local algorithm of ref 28 are also suitable.

Figure 1 presents the comparison of the dynamical evolution of our toy KCM with the geometry of its configuration space. TPS was used on the system defined by eq 15 to generate trajectories between the configurations indicated by a star. In Figure 1a we show both a characteristic trajectory (thin red path) and the average over the set of all trajectories obtained via TPS (thick blue path). We also show geodesics (black curves) joining the final configuration to the initial configuration (indicated by a star), and to other configurations along the gradient descent path (indicated by black squares). The solutions to (14) are degenerate: there is one geodesic going left from the initial point and another going right. The distinction depends on the initial conditions on the path. In the TPS simulations, we force the initial displacement to be to the left to obtain a set of trajectories which follows the left-hand geodesics. These are the paths shown in Figure 1, parts a and b. In Figure 1b, we also show the average over a small set of right-hand TPS trajectories and the corresponding pairs of geodesics.

In Figure 1, we see the features described in the previous section. Initially, the system is in the high energy region and it relaxes approximately by gradient descent. As it reaches the region of weak dynamic facilitation at low energies, the system relaxes by following approximately the geodesics of configuration space. Shown for comparison in Figure 1a are the trajectories followed by an unconstrained version of the same model (dashed green path). In this case, relaxation is by gradient descent. Given that the rate for motion in the x (respectively y) direction vanishes when y (respectively x) vanishes, trajectories have to cross the coordinate axis orthogonally, which gives trajectories (and geodesics) a "rectangular" shape. Equipotential lines are concentric circles, and the conflict between allowed dynamical paths and energy relaxation is evident.

4. An Even Simpler Example

We can gain more insight into the nature of dynamic facilitation by considering an even simpler, one-variable model.

This can be thought of as modeling facilitated dynamics for an order parameter, rather than for microscopic variables. Equations 5 and 6 tell us that an N-variable, dynamically constrained system looks like a single particle diffusing in N space dimensions. Thus, a one-variable dynamically constrained model looks like a single particle diffusing in one space dimension. We can exploit the fact that one-dimensional spaces are always flat[24] to "remove" the kinetic constraint. We will see below that this can be done at the expense of introducing an effective free energy barrier.

Consider a model with one degree of freedom, x, with Hamiltonian (1) $H = Jx^2/2$. We choose the dynamical constraint to be $\mathcal{C}(x)$. This differs from the higher-dimensional cases in that the variable constrains itself. Consequently, the transformation from Fokker−Planck to Langevin form is ambiguous[25] and depends on whether one choses pre-point or midpoint discretisation of time-dependent quantities (Itô or Stratonovich calculus). We choose the former, so that our model is causal. The Langevin description of our one-variable model is then

$$\dot{x}(t) = -Jx\mathcal{C}(x) + T\mathcal{C}'(x) + \sqrt{\mathcal{C}(x)}\eta(t) \qquad (16)$$

where the prime denotes differentiation with respect to x, and the noise term $\eta(t)$ has zero mean and variance $\langle \eta(t)\eta(t')\rangle = 2T\delta(t - t')$. Since in this case the constraint depends on the variable it constrains, the second term on the right-hand side of (16) is needed to ensure an equilibrium density proportional to $\exp(-Jx^2/2T)$.[29] In the higher-dimensional cases, we considered above there was no self-facilitation and this term was absent. The corresponding unconstrained model has $\mathcal{C}(x) = 1$, and its Langevin equation is $\dot{x}(t) = -\partial_x(Jx^2/2) + \eta(t)$.

The appearance of the multiplicative noise term $\sqrt{\mathcal{C}(x)}(t)$ in eq 16 is due to the metric-augmented diffusion term in (6) and is therefore a consequence of the kinetic constraint. The statement that a one-dimensional space is flat is equivalent to the statement that the noise may be made additive by a local change of variables. If we make the change of variables

$$y(t) \equiv \int^{x(t)} \frac{dx'}{\sqrt{\mathcal{C}(x')}} \qquad (17)$$

we can use Itô's formula[25] to rewrite (16) as

$$\dot{y}(t) = -Jx\sqrt{\mathcal{C}(x)} + \frac{1}{2}T\sqrt{\mathcal{C}(x)}\partial_x \ln \mathcal{C}(x) + \tilde{\eta}(t) \qquad (18)$$

where x should be eliminated in favor of y. The noise $\tilde{\eta}(t)$ has the same mean and variance as $\eta(t)$. Provided we can write the deterministic terms in (18) as the gradient of an effective potential, we can regard eq 18 as unconstrained, in the sense that the prefactor of the noise does not contain the dependent variable.

Consider the specific case of a quadratic constraint, $\mathcal{C}(x) = x^2$. Equation (16) becomes

$$\dot{x} = -Jx^3 + 2Tx + x\eta \qquad (19)$$

where we have assumed $x > 0$. The change of variables (17) now amounts to a Cole−Hopf transformation, $y \equiv \ln x$. Hence, the regime where dynamic facilitation is relevant corresponds to $y \ll 0$. Equation 18 now reads

$$\dot{y} = -\partial_y\left(\frac{J}{2}e^{2y} - Ty\right) + \tilde{\eta}. \qquad (20)$$

Equation 20 looks like an unconstrained model with an effective

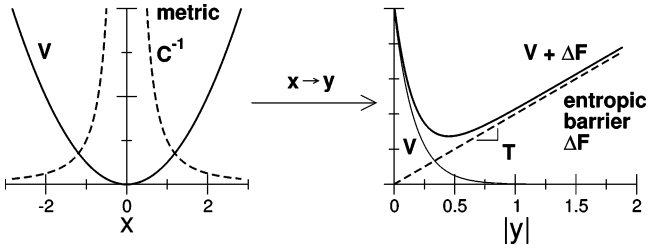

Figure 2. Illustration of how a constrained problem may have an alternative representation as an unconstrained one with an extra free energy barrier (from the example of section 4). The constraint $\mathcal{C}(x)$ fixes the metric $g(x) = \mathcal{C}^{-1}(x)$ of space x. This implies that metric distances become large in the region of small x. Under the transformation eq 17, the problem changes into a non constrained one, $g(y) = 1$, but with an extra free energy barrier $\Delta F(y)$ which excludes the system from the low energy region of large $|y|$.

entropic barrier $\Delta F = -Ty = -T\ln x$, which prevents the particle from accessing the dynamically constrained regime of $y \ll 0 \Rightarrow x \sim 0$.[30] Figure 2 illustrates this.

5. Conclusions

In this paper, we have presented a geometric interpretation of dynamic facilitation. By generalizing kinetically constrained models to continuous degrees of freedom, we have shown that in these systems the kinetic constraints can be seen as endowing configuration space with a nontrivial metric structure. This metric structure in turn determines the dynamical trajectories. In the regime where the kinetic constraint is dominant, i.e., at low temperatures or energies, the geometry forces the dynamics to proceed through paths close to geodesics, rather than close to paths which relax the energy. This conflict between available paths and energy relaxation gives rise to dynamical bottlenecks or barriers, despite the fact that there are no static barriers in these systems.

Our view of dynamical arrest in terms of the geometry of configuration space is distinct from that based on the idea of motion in an effective rugged energy (or free energy) landscape (see ref 3 and references therein). In the landscape perspective, it is often assumed that relevant features of the energy surface, like local minima and saddle points, determine the behavior of the system and that knowledge of the statistical properties of these features is sufficient to explain both dynamic and thermodynamic properties. In our approach, the effective energy surface displays no particular features, the thermodynamics is uninteresting, and there are no special configurations, such as local minima or saddles, which play any major roles either in the statics or in the dynamics. All of the interesting structure is in the paths between configurations and, therefore, in the dynamics. In this picture, it is the effective metric structure of configuration space that distinguishes a glassy system from a normal one and not the ruggedness of its energy surface.

Acknowledgment. We are grateful to D. Chandler for discussions. We acknowledge financial support from EPSRC Grant Nos. GR/R83712/01 and GR/S54074/01, the Glasstone Fund and Linacre College Oxford.

References and Notes

(1) Angell, C. A. *Science* **1995**, *267*, 1924.
(2) Ediger, M. D.; Angell, C. A.; Nagel, S. R. *J. Phys. Chem.* **1996**, *100*, 13200.
(3) Debenedetti, P. G.; Stillinger, F. H. *Nature* **2001**, *410*, 259.

(4) Garrahan, J. P.; Chandler, D. *Phys. Rev. Lett.* **2002**, *89*, 035704; *Proc. Natl. Acad. Sci. U.S.A.* **2003**, *100*, 9710.
(5) Berthier, L.; Garrahan, J. P. *J. Chem. Phys.* **2003**, *119*, 4367; *Phys. Rev. E* **2003**, *68*, 041201.
(6) Whitelam, S.; Berthier, L.; Garrahan, J. P. e-print cond-mat/0310207, 2003.
(7) Berthier, L. e-print cond-mat/0310210, 2003.
(8) Jung, Y.; Garrahan, J. P.; Chandler, D. e-print cond-mat/0311396, 2003.
(9) Sillescu, H. *J. Non-Cryst. Solids* **1999**, *243*, 81.
(10) Ediger, M. D. *Annu. Rev. Phys. Chem.* **2000**, *51*, 99.
(11) Glotzer, S. C. *J. Non-Cryst. Solids* **2000**, *274*, 342.
(12) Schmidt-Rohr, K.; Speiss, H. *Phys. Rev. Lett.* **1991**, *66*, 3020. M. T. Cicerone Ediger, M. D. *J. Chem. Phys.* **1995**, *103*, 5684. Russell, E. V.; et al. *Phys. Rev. Lett.* **1998**, *81*, 1461. Deschenes, L. A.; Vanden Bout, D. A. *Science* **2001**, *292*, 255.
(13) Muranaka, T.; Hitawari, Y. *Phys. Rev. E* **1995**, *51*, R2735. Perera, D.; Harrowell, P. *Phys. Rev. E* **1995**, *51*, 314. Doliwa, B.; Heuer, A. *Phys. Rev. Lett.* **1998**, *80*, 4915. Donati, C.; et al. *Phys. Rev. E* **1999**, *60*, 3107.
(14) Weeks, E.; et al. *Science* **2000**, *287*, 627.
(15) Glarum, S. H. *J. Chem. Phys.* **1960**, *33*, 639.
(16) Palmer, R.; Stein, D. L.; Abrahams, E.; Anderson, P. W. *Phys. Rev. Lett.* **1984**, *53*, 958.
(17) Fredrickson, G. H.; Andersen, H. C. *Phys. Rev. Lett.* **1984**, *53*, 1244.
(18) Ritort, F.; Sollich, P. *Adv. in Phys.* **2003**, *52*, 219.
(19) Jäckle, J.; Eisinger, S. *Z. Phys.* **1991**, *B84*, 115.
(20) Kob, W.; Andersen, H. C. *Phys. Rev. E* **1993**, *48*, 4364.
(21) For other perspectives on glassiness also based on curved spaces, but with a different microscopic origin, see for example: Steinhardt, P. J.; Nelson, D. R.; Ronchetti, M. *Phys. Rev. Lett.* **1981**, *47*, 1297. Nelson, D. R. *Phys. Rev. B* **1983**, *28*, 5515.
(22) Risken, H. *The Fokker−Planck equation: Methods of solution and Application;* Springer-Verlag: New York, 1984.
(23) Zinn-Justin, J. *Quantum Field Theory and Critical Phenomena*; Oxford University Press: Oxford, U.K., 1989.
(24) Misner, C. W.; Thorne, K. S.; Wheeler, J. A. *Gravitation*; W. H. Freeman and Company: San Francisco, CA, 1973.
(25) Van Kempen, N. G. *Stochastic Processes in Physics and Chemistry*; North-Holland: Amsterdam, 2001.
(26) Bolhuis, P. G.; Chandler, D.; Dellago, C.; Geissler, P. L. *Annu. Rev. Phys. Chem.* **2002**, *59*, 291.
(27) Crooks, G. E.; Chandler, D. *Phys. Rev. E* **2001**, *64*, 026109.
(28) Pratt, L. R. *J. Chem. Phys.* **1986**, *85*, 5045.
(29) In the Itô convention, the Fokker−Planck equation for the Langevin equation 16 is $\partial_t P(x,t) = \partial_x[Jx\mathcal{C}(x)P(x,t) - T\mathcal{C}'(x)P(x,t)] + T\partial^2_x[\mathcal{C}(x)P(x,t)]$. The right-hand side of this equation can be rewritten as $\partial_x\{\mathcal{C}(x)[JxP(x,t) + T\partial_x P(x,t)]\}$, leading to the equilibrium density $P_{eq.}(x) \propto \exp(-Jx^2/2T)$, which is indeed independent of the constraining function $\mathcal{C}(x)$. If the Stratonovich convention is used, the second term in the right-hand side of eq 16 is then preceded by a factor 1/2, giving the same Fokker−Planck equation as above.
(30) The equilibrium density in the y representation is $P_{eq.}(y) \propto \exp(-Je^{2y}/2T + y)$. This corresponds to the density $P_{eq.}(x)$ after the change of variables $x \rightarrow y = \ln x$, as can be seen from the invariance of the partition function: $Z = \int \exp(-Jx^2/2T)\,dx = \int \exp(-Je^{2y}/2T)e^y\,dy$.